RESEARCH ARTICLE
SPACE PHYSICS: IONOSPHERIC PHYSICS

Earth and Planetary Physics
7: 247–256, 2023
doi: 10.26464/epp2023029

Comparison of the reaction of polar mesosphere winter echoes and polar mesosphere summer echoes to high-frequency heating in terms of modulated characteristics

Safi Ullah[1], HaiLong Li[1*], Abdur Rauf[1], Shahid Ullah Khan[2], Sufyan Ullah Khan[3], ShuCan Ge[1,4], Bin Wang[1], MaoYan Wang[5], and Lin Meng[1]

[1]School of Electronic Science and Engineering, University of Electronic Science and Technology of China, Chengdu 610054, China;

[2]Department of Physics, Riphah International University Islamabad Campus, Islamabad 45210, Pakistan;

[3]Department of Physics, University of Science and Technology Bannu, Bannu 28101, Pakistan;

[4]National Key Laboratory of Electromagnetic Environment, China Research Institute of Radiowave Propagation, Qingdao 266107, China;

[5]School of Physics, University of Electronic Science and Technology of China, Chengdu 610054, China

Key Points:

- High-frequency (HF) heating effects on polar mesosphere winter echoes (PMWE) and polar mesosphere summer echoes (PMSE) show a similar heating pattern.
- The main difference is that, as compared with PMWE, PMSE are greatly affected by HF heating. As a result, the modulated characteristics (i.e., recovery and overshoot) produced in PMSE are also greater than those produced in PMWE.

Citation: Ullah, S., Li, H. L., Rauf, A., Khan, S. U., Khan, S. U., Ge, S. C., Wang, B., Wang, M. Y., and Meng, L. (2023). Comparison of the reaction of polar mesosphere winter echoes and polar mesosphere summer echoes to high-frequency heating in terms of modulated characteristics. *Earth Planet. Phys.*, *7*(2), 247–256. http://doi.org/10.26464/epp2023029

Abstract: In this work, for the first time, we have analyzed and compared the responses of polar mesosphere winter echoes (PMWE) and their summer counterpart, polar mesosphere summer echoes (PMSE), to high-frequency (HF) heating in terms of modulated characteristics (i.e., backscatter intensity reduction, recovery, and overshoot). Both PMWE and PMSE observations were from the same site (Tromsø, Norway; 69.6°N, 19.2°E) and radar (EISCAT [European Incoherent Scatter Scientific Association] very high frequency, 224 MHz). The heating patterns of both PMWE and PMSE were found to be similar; however, PMSE was more greatly affected by HF heating. Polar mesosphere summer echoes showed recovery and overshoot more frequently than did PMWE. In addition, the mean recovery and overshoot of PMSE were greater than those of PMWE. The associated electron temperature enhancement was estimated for both PMWE and PMSE and showed that, compared with PMWE, the electron temperature enhancement was more significant in PMSE. The strong heating effects on PMSE may be due to the considerable increase in electron temperature.

Keywords: polar mesosphere winter echo; polar mesosphere summer echo; electromagnetic wave; heating experiment; dusty plasma; ionosphere

1. Introduction

During the winter months (September to April), interesting radar echoes are observed in polar regions at an altitude around 50–80 km, which are called polar mesosphere winter echoes, or PMWE. These fascinating radar echoes can also be observed at the mid-latitudes but less frequently (Czechowsky et al., 1979; Zeller et al., 2006). Polar mesosphere winter echoes occur at lower altitudes than their summer counterparts, which are called polar mesospheric summer echoes, or PMSE (Kirkwood et al., 2013, 2015).

Polar mesospheric summer echoes are an interesting radar phenomenon that occurs in the coldest part of the mesosphere in the summer months (May to August) between 80 and 90 km (von Zahn and Meyer, 1989). One of the fascinating properties of the PMSE are that they often occur in the form of two, three, or many layers. Ge SC et al. (2021) used the PMSE observations of European Incoherent Scatter Scientific Association (EISCAT) very high frequency (VHF) radar and analyzed the characteristics of the layered structure of PMSE. The PMWE morphology showed that they usually occur as multiple echo layers at vertical intervals of several kilometers. Their daily occurrence rate around local noon is high (up to 30%); however, their nighttime occurrence requires strongly disturbed conditions, in which the upper mesosphere must be strongly ionized (e.g., due to geomagnetic activities; Nishiyama et al., 2018). For radar of the same frequency, PMWE, as compared with PMSE, are a rare phenomenon. For example, at

Correspondence to: H. L. Li, hailong703@163.com
Received 09 SEP 2022; Accepted 04 DEC 2022.
Accepted article online 09 FEB 2023.

53.5 MHz radar, the occurrence rates of PMWE and PMSE are a few percent and 80%–90%, respectively (Bremer et al., 2003; Zeller et al., 2006). So far, the main features of PMWE are not understood well and are still under investigation.

The PMWE occurrence rate has a strong positive correlation with the ionization level of the D-region. The literature reveals that the required condition for the existence of PMWE is a high ionization level in the D-region, which is produced because of high energetic particle precipitation, including proton, electron, or enhanced X-ray fluxes (Zeller et al., 2006). In contrast, for the occurrence of PMSE, the presence of energetic particle precipitations is not a necessary condition (Rauf et al., 2018, 2019). In the literature on PMWE, few hypotheses have been advanced on the still unknown mechanism of PMWE generation. Lübken et al. (2006) proposed that layered neutral turbulence, which is excited because of wind shear, can explain PMWE. In mesosphere, the gravity waves generations is presented in Shi GC et al. (2021). The breaking of gravity waves along with the turbulence is considered the main source of PMWE generation. Rapp et al. (2011) showed the relationship of PMWE with the breaking of gravity waves that generate turbulence, whereas Belova et al. (2005) claimed that neutral turbulence alone cannot provide a good explanation for the characteristics of PMWE. The latter claim is supported by the close similarity found in the spectral widths of the PMWE source region (Kirkwood et al., 2006; Zeller et al., 2006). As explained, some hypotheses consider only the turbulence behind the PMWE phenomenon; however, in the PMWE region, the presence of nanometer-sized charged dust particles have also been found in radar and rocket observations (Baumann et al., 2013). Lübken et al. (2006) argued that mesospheric smoke particles may influence electron density fluctuations through charging and consequently produce the radar echoes. Havnes and Kassa (2009) proposed that mesospheric smoke particles that exist in the PMWE source region cause electron irregularities and hence produce the PMWE. However, PMSE are produced because of electron irregularities that are the result of free electrons and ions attaching to nanometer-sized dust particles present in the mesosphere. Compared with PMWE, PMSE have been extensively studied and are a well-understood phenomenon. A review of ionospheric irregularities at mid-latitudes can be found in Liu Y et al. (2021). A statistical analysis of the characteristics of irregular Es layers can be found in Li HL et al. (2021). The irregular Es layers are also called PMSE-like or PMSE-Es (Polar Mesosphere Summer Echoes-Es). For a detailed explanation of PMSE, the reader is referred to the review of Rapp and Lübken (2004).

Artificial electron heating experiments, in which PMSE or PMWE are artificially heated by heating the electrons in the PMSE or PMWE source region with powerful high-frequency (HF) radio waves, are used to diagnose dusty plasmas in the mesosphere (Havnes et al., 2003; Kavanagh et al., 2006). In these experiments, as a result of HF heating, the variation produced in the backscatter intensity profile during a heater on/off cycle, called an overshoot characteristic curve, or OCC, contains information about the dusty plasmas in the mesosphere (Havnes et al., 2003). Using the PMSE observations of the EISCAT VHF radar, Chilson et al. (2000) presented the first study of the HF heating effects on PMSE. Since then, the heating effects on PMSE have been studied extensively with computational models and through experimental observations (e.g., Havnes et al., 2003, 2015; Kassa et al., 2005; Biebricher et al., 2006; Scales and Chen C, 2008; Senior et al., 2014). In contrast, Kavanagh et al. (2006) first presented the heating effects on PMWE by using the PMWE observations of the EISCAT VHF radar with a 10 s heating cycle. Belova et al. (2008) extended this study by using the PMWE observations of the same VHF radar, but with a different heating cycle (on/off, 20 s/160 s). Further experimental studies include La Hoz and Havnes (2008), in which the heating effects on PMWE were studied by using the observations of mesosphere–stratosphere–troposphere Mobile Rocket and Radar Observatory (MST MORRO) 56 MHz radar. Using the PMWE observations of the same MST MORRO radar, Havnes et al. (2011) showed a small recovery in intensity during the heater-on time and an increase in intensity after the heater-off time. Both of these effects were attributed to dust charging, in which the charging of free electrons onto dust particles took place as a result of the electron temperature enhancement caused by heating. Kero et al. (2008) found the signature of negatively charged dust particles by using the observations and the Sodankylä Ion Chemistry (SIC) model, in which the electron density variation was compared between the heater-on and heater-off periods.

The presented literature on PMSE and PMWE lacks a direct and detailed comparison of the heating effects of PMSE and PMWE in terms of modulated characteristics (i.e., backscatter intensity reduction, recovery, and overshoot). In this work, for the first time, we analyze and compare the responses of PMSE and PMWE to HF heating in terms of modulated characteristics. To obtain important information about the physics of the heating mechanism of the radar echoes, we mainly focus on the differences and similarities between the results. We believe this statistical analysis sheds further light on the HF heating effects on PMSE and PMWE.

2. Experimental Description

The measurements analyzed in this study were performed in the winter and summer seasons with EISCAT VHF (224 MHz) radar. The PMWE and PMSE observations used in the study are shown in Tables 1 and 2, respectively. The second column of Tables 1 and 2 states only when PMWE and PMSE were observed; it does not show the exact duration of the PMWE and PMSE events. A detailed description of VHF radar can be found in Baron (1986). For heating of PMWE and PMSE, the EISCAT HF Heating facility (commonly known as Heating; Rietveld et al., 1993, 2016; Rietveld and Stubbe, 2022) co-located at the EISCAT site was also operating during the experiments with different frequencies and polarization modes, as shown in Tables 1 and 2, respectively.

3. Data Analysis

The EISCAT analysis tool GUISDAP (the Grand Unified Incoherent Scatter Design and Analysis Program; Lehtinen and Huuskonen, 1996) was used to analyze the raw electron density. The "apparent" electron number density can be converted into volume reflectivity, η. Volume reflectivity is the radar-scattering cross section per unit volume, indicating the absolute strength of the radar echoes. It can be derived from the well-known relation as

$$\eta = \sigma \times N_e, \tag{1}$$

where σ is half the radar-scattering cross section of an electron,

Table 1. Details of polar mesosphere winter echo observations with EISCAT very high frequency 224 MHz radar.

Date	Time (UT)	On/off cycle (s)	Integration time (s)	Experiment	Polarization (mode)	Heater frequency (MHz)
2006-10-24	11:00–12:00	20/160	2	arc_dlayer	X	5.423
2006-11-24	08:30–09:03	20/160	2	arc_dlayer	X	5.423
2006-11-24	09:50–10:25	20/160	2	arc_dlayer	X	5.423
2006-11-27	11:05–11:45	20/160	2	arc_dlayer	O	5.423
2008-02-05	09:45–10:45	06/06	2	arc_dlayer	X	5.423
2012-02-28	09:00–11:30	24/96	4.8	manda	X	7.953
2014-02-20	10:00–11:30	48/144	4.8	manda	X	5.423

Table 2. Details of polar mesosphere summer echo observations with EISCAT very high frequency 224 MHz radar.

Date	Time (UT)	On/off cycle (s)	Integration time (s)	Experiment	Polarization (mode)	Heater frequency (MHz)
2004-07-15	07:24–11:24	20/160	2	arc_dlayer	X	5.423
2007-07-13	09:00–13:00	20/160	2	arc_dlayer_ht	O	5.423
2013-07-26	09:00–13:00	48/168	4.8	manda	O	6.77

numerically equal to 4.99×10^{-29} m^2, and N_e is the "apparent" electron density (Röttger and La Hoz, 1990).

To detect PMWE and to minimize the effect of random statistical fluctuations in addition to the contribution from noise, each data set was divided into segments of one-hour duration. Then, for each height, only those heating cycles were selected in which PMWE were present. The presence of PMWE for any heating cycle was considered only when one data point before the heater switch-on was satisfying the threshold, $\eta \geq 1.3 \times 10^{-19}$ m^{-1}. In this way, PMWE were detected for different heating cycles between 56 and 80 km. Polar mesosphere winter echo observations are rare, especially in combination with heating; therefore, to avoid poor statistics (only a few cycles), we considered the total observations shown in Table 1. On the basis of the PMWE threshold of this paper, 40 heating cycles were selected from the observations shown in Table 1. For comparison with PMWE, we also used the PMSE observations shown in Table 2. In the case of PMSE, for heating cycles between 80 and 90 km, the heating cycles considered to have PMSE were only those in which one data point before the heater turn-on was satisfying the threshold, $\eta \geq 5 \times 10^{-18}$ m^{-1}. For comparison, PMSE observations were selected from different days and years. Polar mesosphere summer echo observations at VHF radar are not rare; therefore, 40 heating cycles were selected from each date shown in Table 2. For good comparison, the PMSE and PMWE observations should be from the same site, radar, time, and height. However, in this work we used only observations from the same site (Tromsø EISCAT, 69.6°N, 19.2°E) and radar (VHF, 224 MHz) because different seasonal (winter and summer) observations from the same time are impossible. Similarly, PMWE occur below the altitude of PMSE; therefore, selecting observations from the

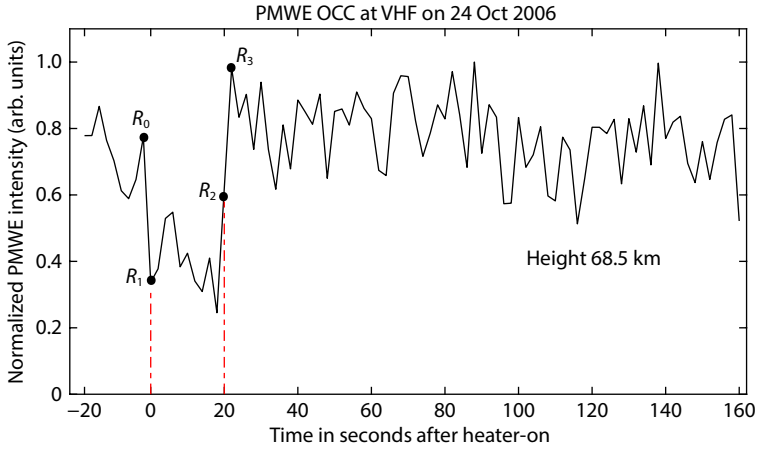

Figure 1. Overshoot characteristic curve (OCC) showing the parameters R_0, R_1, R_2, and R_3, where R_0 is the PMWE intensity before the heater-on time; R_1 is after the heater-on time; R_2 is before the heater-off time, and R_3 is after the heater-off time. The normalization of the polar mesosphere winter echo (PMWE) intensity was done by dividing each data point of the heating cycle by the maximum value of the cycle. The large black circles are used to identify the positions of the OCC parameters. The heater is on for 20 s from 11:36:00 UT on October 24, 2006, where the heating pulse occurs between the vertical lines at 0 and 20 s. VHF, very high frequency.

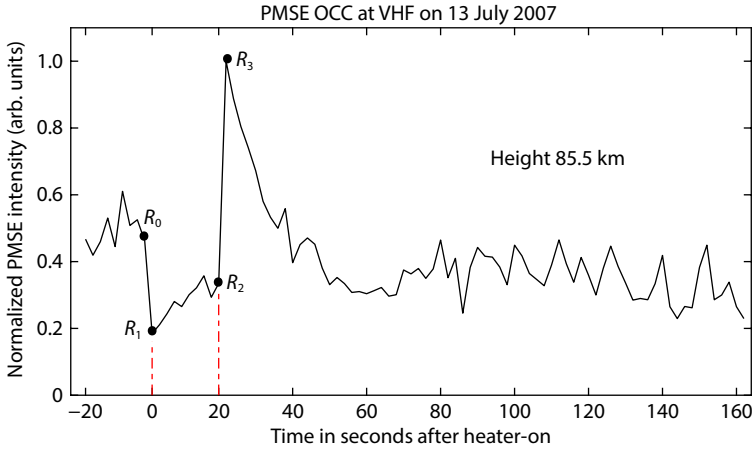

Figure 2. Same as Figure 1 but for polar mesosphere summer echoes (PMSE), where the heater is on for 20 s from 11:30:00 UT on July 13, 2007.

same height is also impossible.

4. Method Used for Calculation of the OCC Parameters

Figures 1 and 2 present an example of PMWE and PMSE profiles, respectively, showing the heater-induced variations. In both PMWE and PMSE, a clear change can be seen during the heater-on time (0–20 s). The main regions of the PMWE and PMSE that interact with the heater wave at different time intervals are identified with the parameters R_0, R_1, R_2, and R_3, called the OCC parameters. These parameters represent the PMWE or PMSE intensity as follows: R_0, before the HF heater-on time; R_1, after the HF heater-on time; R_2, before the HF heater-off time, and R_3, after the HF heater-off time. Using the observations presented in Tables 1 and 2, we calculated these parameters for PMWE and PMSE.

5. Results and Discussion

In the present work, we used the OCC parameters for analysis. The ratio between different OCC parameters showed variation in the PMSE or PMWE intensity caused by HF heating. The variations from different pairs gave different characteristics, normally known as modulated characteristics of PMSE or PMWE. In this section, we compare the heating effects on radar echoes in terms of modulated characteristics between the PMWE and PMSE.

5.1 Comparison of R_1/R_0 Between PMSE and PMWE

Figure 3 shows a comparison of the immediate response of the radar backscatter to the HF heater being turned on in the winter and summer seasons. The ratio $R_1/R_0 > 1$ is called an onset overshoot, whereas $R_1/R_0 < 1$ represents the backscatter intensity reduction resulting from HF heating. We see that both PMWE and PMSE experienced no onset overshoot ($R_1/R_0 > 1$) but instead showed a reduction ($R_1/R_0 < 1$). The abrupt weakening of the PMSE and PMWE just after the heater was turned on had the same cause. The intensity of both PMSE and PMWE was decreased because of a diffusion of electrons and ions as the considerable enhancement in electron temperature reduced the electron density gradients that produce the observed radar backscatter (La Hoz and Havnes, 2008). The result shown in Figure 3 is in agreement with the present literature on PMSE and PMWE (Chilson et al., 2000; Havnes et al., 2003, 2015; Kavanagh et al., 2006; Belova et al., 2008; La Hoz and Havnes, 2008; Næsheim et al., 2008), where for a VHF of 224 MHz radar, the onset overshoot has not been observed. The onset overshoot is possible for low-frequency radar, as predicted by Scales (2004) and as shown experimentally for PMSE by Havnes et al. (2015) for 56 MHz radar. Senior et al. (2014) showed an example of onset overshoot for PMSE at VHF 224 MHz radar; however, the literature on PMSE and PMWE reveals that for VHF 224 MHz radar, onset overshoot is very rare and normally the PMSE or PMWE intensity decreases when it interacts with the

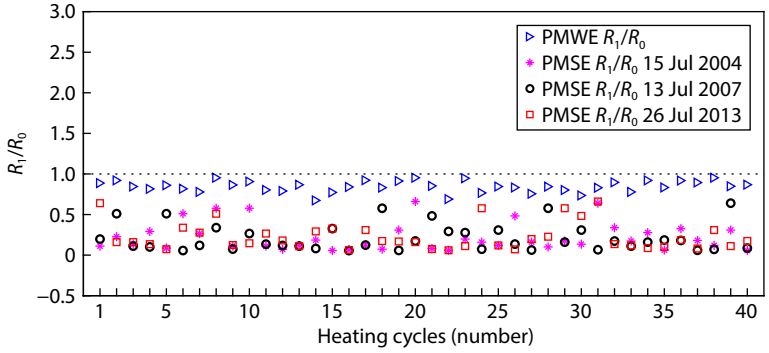

Figure 3. Comparison of ratio R_1/R_0 between polar mesosphere summer echoes (PMSE) and polar mesosphere winter echoes (PMWE). The PMWE data points (values of the ratio R_1/R_0) are from the observations shown in Table 1, whereas the PMSE observations are from Table 2. The ratio $R_1/R_0 > 1$ shows onset overshoot, whereas $R_1/R_0 < 1$ shows a backscatter intensity reduction resulting from heating. The ratio $R_1/R_0 = 1$ is represented by the horizontal dotted line, indicating no heating effect.

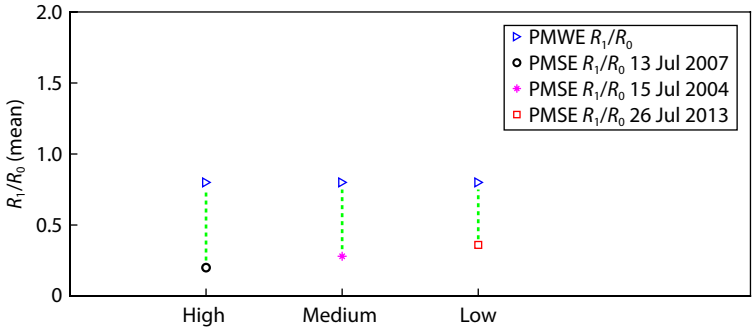

Figure 4. Comparison of means of R_1/R_0 between polar mesosphere winter echoes (PMWE) and polar mesosphere summer echoes (PMSE). The vertical dotted line is used only to show the difference between the mean values of PMSE and PMWE.

heater wave. For further explanation, we plotted the mean values of the ratio R_1/R_0, as shown in Figure 4. It is clear that for PMWE, the mean of ratio R_1/R_0 is larger than that for PMSE. This result indicates that PMWE decreases less after the heater is switched on, whereas for PMSE, the smaller values of R_1/R_0 mean that the PMSE intensity decreases more and that the heating effect on PMSE is stronger.

5.2 Comparison of R_2/R_0 Between PMSE and PMWE

The response of PMSE and PMWE to HF heating in the second stage of OCC is shown in Figure 5. The ratio $R_2/R_0 > 1$ or $R_2 > R_0$ is defined as backscatter intensity recovery during the heater-on time (Havnes et al., 2015). It is clear that PMSE observations show recovery far more often than PMWE observations. This result is further explained in Figure 6, where in the upper panel, we demonstrate the percentage of recovery for PMSE and PMWE. The percentage of recovery is obtained by dividing the number of heating cycles having recovery to the total number of heating cycles times 100. It is clear that the percentage of PMSE recovery is greater than the percentage of PMWE recovery. For PMSE, a considerable number of heating cycles show recovery, whereas for PMWE, only a few cycles (10%) show recovery. Similarly, in the lower panel of Figure 6, the mean values of recovery for PMSE are larger than those for PMWE. This result means that the recovery produced in radar backscatter in the summer months is greater than that produced in the winter months.

The presence of charged dust particles causes the recovery of PMSE and PMWE because during the heater-on phase, when the dust particles are charged up, it consequently increases the gradients in the electron irregularities (Havnes et al., 2004). This qualitative description of the role of charged dust particles in recovery has also been confirmed in model studies (Havnes et al., 2003; Havnes, 2004; Biebricher et al., 2006). Here, it is clear that in the case of PMWE, most of the heating cycles show no recovery during the heater-on periods. This result suggests the presence of very small dust particles with a radius less than 10 nm (Havnes et al., 2004; Havnes and Kassa, 2009).

5.3 Comparison of R_3/R_0 Between PMSE and PMWE

The response of PMSE and PMWE to HF heating in the third stage of OCC is shown in Figure 7. The ratio $R_3/R_0 > 1$ or $R_3 > R_0$ is defined as the backscatter intensity overshoot that takes place just after the heater is turned off (Havnes et al., 2015). It is clear that in the case of PMSE, overshoot is present for a greater number of cycles, whereas for PMWE, only a few heating cycles show clear overshoot. From Figure 8 (upper panel), we can see that the percentage of overshoot is greater for PMSE than for PMWE. This means that for PMSE, the production rate of overshoot is greater than for PMWE. Similarly, from Figure 8 (lower panel), we can see that the mean values of overshoot for PMSE are larger than those for PMWE. This means that the PMSE overshoot is greater than the PMWE overshoot.

Polar mesosphere summer echoes contain comparatively large and visually observable dust particles of sizes from ~10 to ~100 nm (von Cossart et al., 1999), whereas PMWE contain very small dust particles of sizes from ~3 to ~4 nm and smaller, which are not

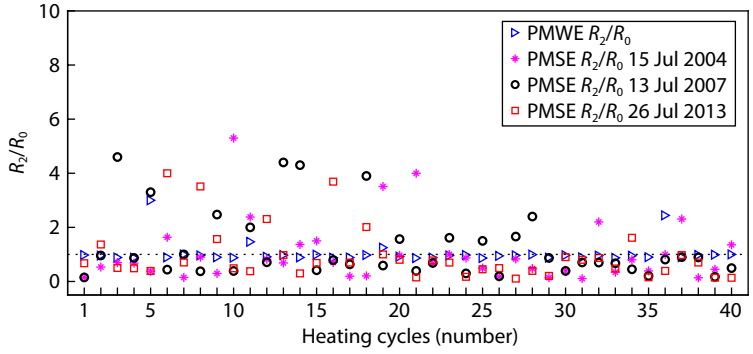

Figure 5. The same as for Figure 3 but for overshoot characteristic curve (OCC) parameters R_2 and R_0. The ratio $R_2/R_0 > 1$ is characterized as polar mesosphere summer echo (PMSE) or polar mesosphere winter echo (PMWE) intensity recovery.

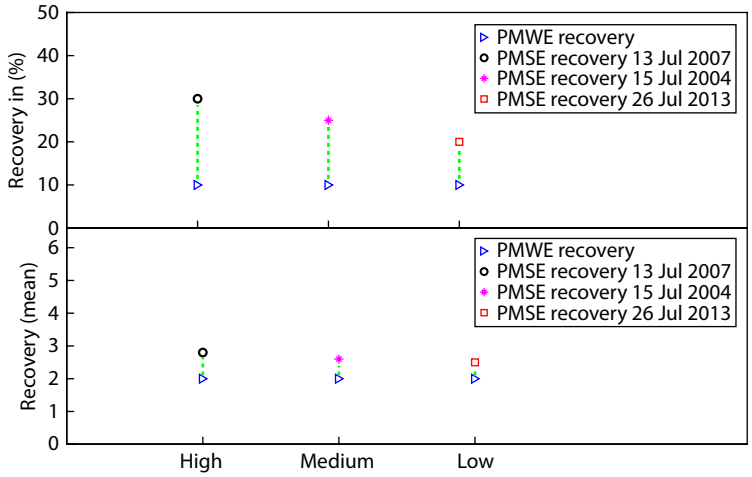

Figure 6. (Upper panel) Comparison of the percentage of recovery between polar mesosphere summer echoes (PMSE) and polar mesosphere winter echoes (PMWE). The percentage values of recovery were obtained by dividing the number of heating cycles having recovery to the total number of heating cycles times 100. (Lower panel) Comparison of the mean recovery between PMSE and PMWE. The vertical dotted line is used only to show the difference between the values of PMSE and PMWE.

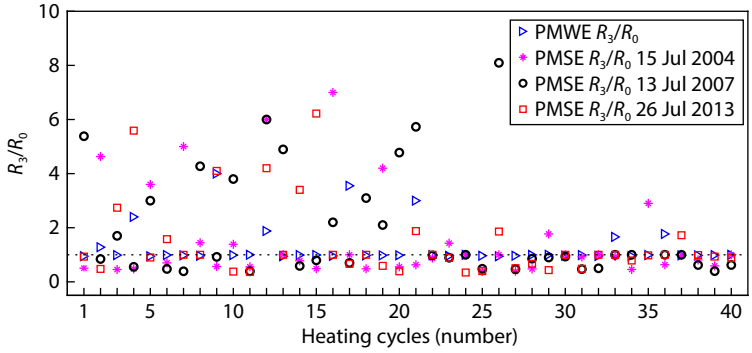

Figure 7. Same as for Figure 3 but for overshoot characteristic curve (OCC) parameters R_3 and R_0. The ratio $R_3/R_0 > 1$ is characterized as the polar mesosphere summer echo (PMSE) or polar mesosphere winter echo (PMWE) intensity overshoot.

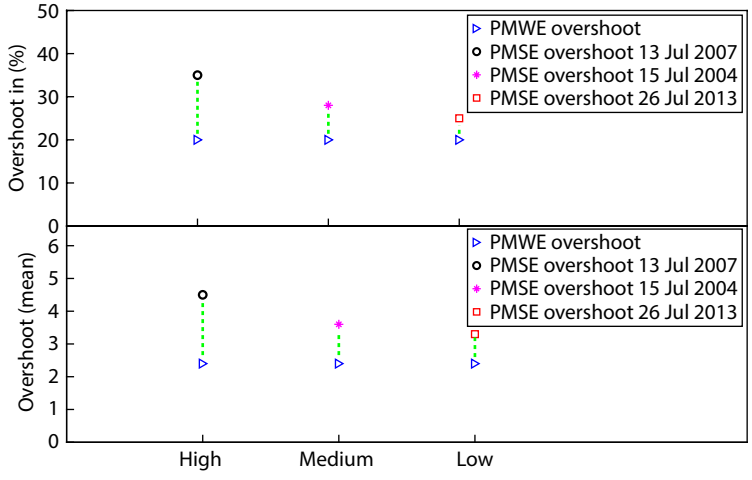

Figure 8. (Upper panel) Comparison of the percentage of overshoot between polar mesosphere summer echoes (PMSE) and polar mesosphere winter echoes (PMWE). The percentage values of overshoot were obtained by dividing the number of heating cycles having overshoot to the total number of heating cycles times 100. (Lower panel) Comparison of the mean overshoot between PMSE and PMWE. The vertical dotted line is used only to show the difference between the values of PMSE and PMWE.

visually observable (Havnes and Kassa, 2009). This is one of the possible reasons we see that the PMSE overshoot is greater than the PMWE overshoot: because the size and density of dust particles play important roles in producing the PMSE or PMWE overshoot. The dust particles gain an additional negative charge during the time the heater is on. This charging of dust particles increases the gradients in electron irregularities and hence causes recovery and overshoot (Havnes et al., 2004).

The weakening of the PMSE intensity just after the heater is turned on, followed by a recovery of intensity during the heater-on phase and a corresponding overshoot of intensity over the background level just after the heater is switched off is in agreement with the existing PMSE literature (Havnes et al., 2003; Havnes, 2004; Biebricher et al., 2006; Næsheim et al., 2008; Pinedo et al., 2014; Ullah et al. 2019). In the case of PMWE, similar behaviors were observed during a heating cycle and are in accordance with the existing literature on PMWE (Kavanagh et al., 2006; La Hoz and Havnes, 2008; Havnes et al., 2011; Mahmoudian et al., 2017). The recovery and overshoot arise because when heated, the electrons increase their incident flux on the PMWE and PMSE dust particles, thus increasing their charge, which in turn strengthens the electron density irregularities. When the heating stops, the dust discharges the extra charge with a characteristic relaxation time before reaching equilibrium. The greater mean recovery and overshoot of PMSE are due to the larger heating effects and dust sizes, which lead to a substantial additional charging of the PMSE dust particles. On the other hand, the small mean recovery and overshoot of PMWE are the result of the small charges and sizes of the PMWE dust particles (La Hoz and Havnes, 2008).

5.4 Comparison of the Modulation Index and Enhanced Electron Temperature Between PMSE and PMWE

The ratio of heated to unheated radar backscatter is called the backscatter modulation index. It describes how much the heated backscattered radar varies with respect to its unheated state. The mathematical equation for the PMSE or PMWE modulation index was first presented by Routledge et al. (2011) and can be written as

$$MI(\%) = ((R_0 - R_1)/R_0) \times 100, \tag{2}$$

where MI is the PMSE or PMWE modulation index, R_0 is the unheated PMSE or PMWE intensity, and R_1 is the heated PMSE or PMWE intensity.

When PMWE or PMSE have a high density of plasma compared with the density of dust, then the expressions linking the enhanced electron temperature and the ratio R_1/R_0 (Havnes et al., 2004; Kassa et al., 2005) can be written as

$$T_e/T_i = \left(2 - \sqrt{R_1/R_0}\right)\Big/\left(\sqrt{R_1/R_0}\right), \tag{3}$$

where T_e is the heated (enhanced) electron temperature attributable to heating and T_i is the unheated ion temperature because ions and neutrals are not affected by the HF heating (Kassa et al., 2005) and their temperatures remains the same ($T_i = T_N = 150$ K).

In the mesosphere, the electron temperature is an important physical parameter that changes because of HF heating and, as a result, produces significant changes in PMSE and PMWE. In Figure 9, we show the modulation indexes (MI) and the corresponding enhanced electron temperatures (T_e/T_i) for PMSE and PMWE. It is obvious that the MI and T_e/T_i for PMSE are greater than those for PMWE. Here, we set $MI > 30\%$ and $T_e/T_i > 5$ as a reference for the purpose of comparing PMSE and PMWE in more detail. Our purpose is to show, among the 40 heating cycles, the number of heating cycles in which the PMSE or PMWE MI is greater than 30% and the number of heating cycles in which the T_e/T_i is enhanced 5 times to its unheated state. This result is shown in Figure 10, where we see that for PMWE, both $MI > 30\%$ and $T_e/T_i > 5$ are 0%. This means that for PMWE, no heating cycle occurs in which, because of heating, PMWE are modulated by 30% to their unheated state; similarly, no heating cycle occurs in which the T_e/T_i is enhanced 5 times to its unheated state. On the other hand, for PMSE, a significant number of heating cycles occur in which,

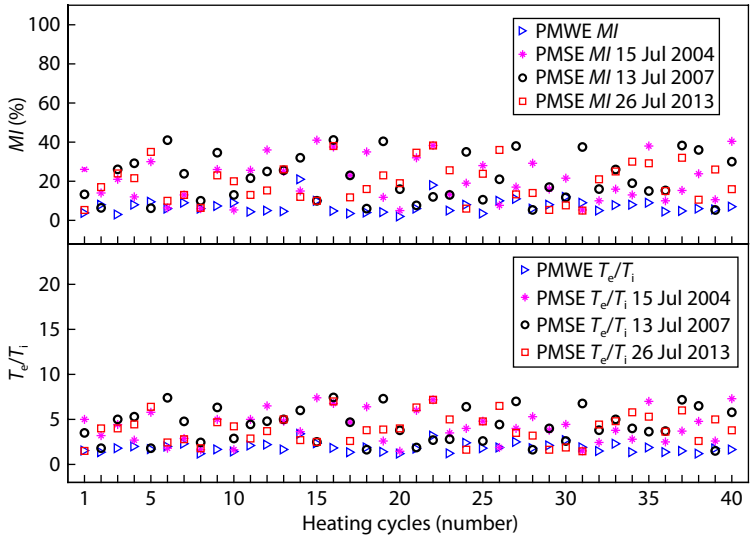

Figure 9. Comparison of (upper panel) the modulation indexes (MI) and (lower panel) the enhanced electron temperatures (T_e/T_i) between polar mesosphere summer echoes (PMSE) and polar mesosphere winter echoes (PMWE).

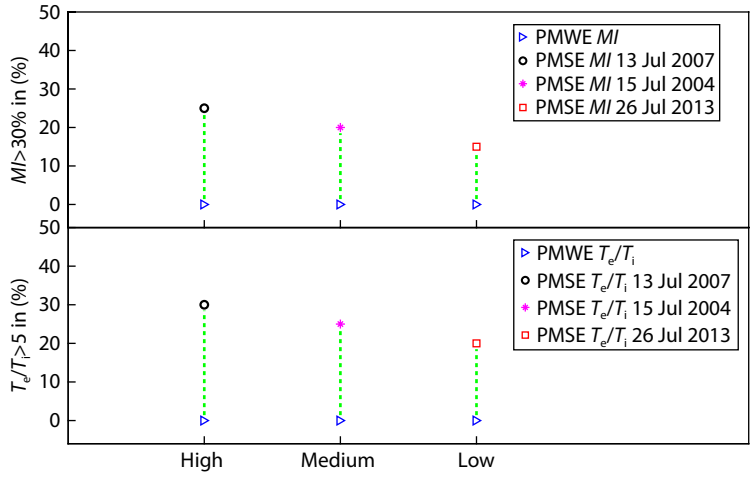

Figure 10. Comparison of the modulation indexes (*MI*) > 30% and the enhanced electron temperatures (T_e/T_i) > 5 as percentages between polar mesosphere summer echoes (PMSE) and polar mesosphere winter echoes (PMWE). The percentage values of *MI* > 30% and T_e/T_i > 5 were obtained by dividing the number of heating cycles having *MI* > 30% and T_e/T_i > 5 to the total number of heating cycles times 100. The vertical dotted line is used only to show the difference between the percentage values of PMSE and PMWE.

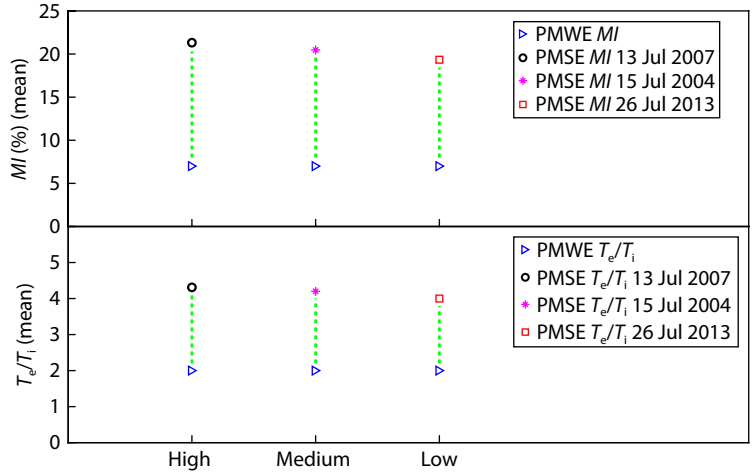

Figure 11. Comparison of means of (upper panel) the modulation indexes (*MI*) and (lower panel) the enhanced electron temperatures (T_e/T_i) between polar mesosphere summer echoes (PMSE) and polar mesosphere winter echoes (PMWE). The vertical dotted line is used only to show the difference between the mean values of PMSE and PMWE.

because of heating, the PMSE is modulated by 30% and the T_e/T_i is enhanced 5 times to its unheated state. For example, on July 13, 2007 (represented by a circle), for PMSE, the *MI* > 30% is 25% (upper panel) and the T_e/T_i > 5 is 30% (lower panel). This means that on July 13, 2007, because of heating, in 25% of the heating cycles, PMSE is modulated by 30% to its unheated state, and among the total 40 heating cycles, in 30% of the cycles, the T_e/T_i is enhanced 5 times to its preheated state. Figure 11 shows the mean values of *MI* and T_e/T_i for PMSE and PMWE. It is clear that for PMSE, both the *MI* and T_e/T_i are greater than those for PMWE. This means that in PMSE, because of HF heating, the greater enhancement of the electron temperature produces a greater modulation in PMSE, whereas in PMWE, the small enhancement in the electron temperature causes only a small modulation in PMWE. In PMSE compared with PMWE, the higher T_e/T_i caused by heating is responsible for producing the higher modulation in PMSE.

Higher electron temperatures are associated with the reduction of PMWE and PMSE. Belova et al. (2001) showed that this relationship is not linear and that it varies with altitude. An additional limitation is that the background electron density levels at lower altitudes determine the electron heating higher up (Pinedo et al., 2014). Polar mesosphere winter echoes occur mainly during disturbed conditions with high electron densities because of energetic particle precipitation (Havnes et al., 2011). In contrast, PMSE do not necessarily occur in the presence of energetic particle precipitation (Rauf et al., 2018, 2019). Therefore, in the case of PMWE with high electron densities in the lower parts, most of the heater wave energy is absorbed and only a small amount reaches the PMWE altitudes, whereas in the case of PMSE with low electron densities below the PMSE altitudes, most of the heater wave energy reaches the PMSE altitudes and heats the PMSE there. Heating the ionosphere with HF radio waves enhances the electron temperature (Chilson et al., 2000; Havnes et al., 2003, 2004, 2011; Kassa et al., 2005; Routledge et al., 2011). Therefore, in the case of PMSE, where enough heater wave energy is available at PMSE altitudes,

the electron temperature is enhanced more significantly than in PMWE. The absorption of the HF wave in the D-region should have a significant impact on the heating of the F-region because the variations in electron density in the D-region affect the electron temperature enhancement. Therefore, the heating effects in the D- and F-regions may be different because of variations in electron density in the D- and F-regions. However, a future detailed study with a larger experimental data set under different conditions would be required to determine this.

6. Conclusions

We have analyzed and compared the PMWE and PMSE observations of VHF (224 MHz) radar modulated by artificial electron heating with the EISCAT HF Heating facility. Our results show that during HF heating, the PMWE and PMSE follow a similar heating pattern but that the HF heating greatly affects the PMSE as compared with the PMWE. Statistics reveal that recovery and overshoot are produced more frequently in PMSE than in PMWE. Similarly, the mean recovery and overshoot in PMSE are greater than those in PMWE. The electron temperature enhancement attributable to heating was estimated and indicated that in the case of PMSE, the electron temperature is greatly enhanced compared with the temperature enhancement in PMWE. This significant enhancement in electron temperature may be responsible for the larger heating effects in PMSE.

Acknowledgments

We thank Ingemar Häggström for helpfulness in providing the experimental information on the heating experiments. We also appreciate the EISCAT, an international association supported by research organizations in China (CRIRP), Finland (SA), Japan (NIPR and ISEE), Norway (NFR), Sweden (VR), and the United Kingdom (UKRI). This work was supported by the National Natural Science Foundation of China (No. 62271113, 62201529), the National Key Laboratory of Electromagnetic Environment (No. 202102010), and the Natural Science Foundation of Sichuan Province (No. 2022NSFSC1848).

References

Baron, M. (1986). EISCAT progress 1983–1985. *J. Atmos. Terr. Phys.*, *48*(9–10), 767–772. https://doi.org/10.1016/0021-9169(86)90050-4

Baumann, C., Rapp, M., Kero, A., and Enell, C. F. (2013). Meteor smoke influences on the D-region charge balance—review of recent in situ measurements and one-dimensional model results. *Ann. Geophys.*, *31*(11), 2049–2062. https://doi.org/10.5194/angeo-31-2049-2013

Belova, E., Chilson, P., Rapp, M., and Kirkwood, S. (2001). Electron temperature dependence of PMSE power: experimental and modelling results. *Adv. Space Res.*, *28*(7), 1077–1082. https://doi.org/10.1016/S0273-1177(01)80040-5

Belova, E., Kirkwood, S., Ekeberg, J., Osepian, A., Häggström, I., Nilsson, H., and Rietveld, M. (2005). The dynamical background of polar mesosphere winter echoes from simultaneous EISCAT and ESRAD observations. *Ann. Geophys.*, *23*(4), 1239–1247. https://doi.org/10.5194/angeo-23-1239-2005

Belova, E., Smirnova, M., Rietveld, M. T., Isham, B., Kirkwood, S., and Sergienko, T. (2008). First observation of the overshoot effect for polar mesosphere winter echoes during radiowave electron temperature modulation. *Geophys. Res. Lett.*, *35*(3), L03110. https://doi.org/10.1029/2007gl032457

Biebricher, A., Havnes, O., Hartquist, T. W., and La Hoz, C. (2006). On the influence of plasma absorption by dust on the PMSE overshoot effect. *Adv. Space Res.*, *38*(11), 2541–2550. https://doi.org/10.1016/j.asr.2005.02.061

Bremer, J., Hoffmann, P., Latteck, R., and Singer, W. (2003). Seasonal and long-term variations of PMSE from VHF radar observations at Andenes, Norway. *J. Geophys. Res.: Atmos.*, *108*(D8), 8438. https://doi.org/10.1029/2002jd002369

Chilson, P. B., Belova, E., Rietveld, M. T., Kirkwood, S., and Hoppe, U. P. (2000). First artificially induced modulation of PMSE using the EISCAT heating facility. *Geophys. Res. Lett.*, *27*(23), 3801–3804. https://doi.org/10.1029/2000GL011897

Czechowsky, P., Rüster, R., and Schmidt, G. (1979). Variations of mesospheric structures in different seasons. *Geophys. Res. Lett.*, *6*(6), 459–462. https://doi.org/10.1029/GL006i006p00459

Ge, S. C., Li, H. L., Xu, B., Xu, T., Meng, L., Wang, M. Y., Hannachi, A., Zhu, M. Y., Broman, L., … Rauf, A. (2021). Characteristic analysis of layered PMSEs measured with different elevation angles at VHF based on an experimental case. *Earth Planet. Phys.*, *5*(1), 42–51. https://doi.org/10.26464/epp2021001

Havnes, O., La Hoz, C., Næsheim, L. I., and Rietveld, M. T. (2003). First observations of the PMSE overshoot effect and its use for investigating the conditions in the summer mesosphere. *Geophys. Res. Lett.*, *30*(23), 2229. https://doi.org/10.1029/2003GL018429

Havnes, O., La Hoz, C., Biebricher, A., Kassa, M., Meseret, T., Næsheim, I., and Zivkovic, T. (2004). Investigation of the mesospheric PMSE conditions by use of the new overshoot effect. *Phys. Scr.*, *2004*(T107), 70. https://doi.org/10.1238/physica.topical.107a00070

Havnes, O. (2004). Polar mesospheric summer echoes (PMSE) overshoot effect due to cycling of artificial electron heating. *J. Geophys. Res.: Space Phys.*, *109*(A2), A02309. https://doi.org/10.1029/2003JA010159

Havnes, O., and Kassa, M. (2009). On the sizes and observable effects of dust particles in polar mesospheric winter echoes. *J. Geophys. Res.: Atmos.*, *114*(D9), D09209. https://doi.org/10.1029/2008jd011276

Havnes, O., La Hoz, C., Rietveld, M. T., Kassa, M., Baroni, G., and Biebricher, A. (2011). Dust charging and density conditions deduced from observations of PMWE modulated by artificial electron heating. *J. Geophys. Res.: Atmos.*, *116*(D24), D24203. https://doi.org/10.1029/2011jd016411

Havnes, O., Pinedo, H., La Hoz, C., Senior, A., Hartquist, T. W., Rietveld, M. T., and Kosch, M. J. (2015). A comparison of overshoot modelling with observations of polar mesospheric summer echoes at radar frequencies of 56 and 224 MHz. *Ann. Geophys.*, *33*(6), 737–747. https://doi.org/10.5194/angeo-33-737-2015

Kassa, M., Havnes, O., and Belova, E. (2005). The effect of electron bite-outs on artificial electron heating and the PMSE overshoot. *Ann. Geophys.*, *23*(12), 3633–3643. https://doi.org/10.5194/angeo-23-3633-2005

Kavanagh, A. J., Honary, F., Rietveld, M. T., and Senior, A. (2006). First observations of the artificial modulation of polar mesospheric winter echoes. *Geophys. Res. Lett.*, *33*(19), L19801. https://doi.org/10.1029/2006gl027565

Kero, A., Enell, C. F., Kavanagh, A. J., Vierinen, J., Virtanen, I., and Turunen, E. (2008). Could negative ion production explain the polar mesosphere winter echo (PMWE) modulation in active HF heating experiments?. *Geophys. Res. Lett.*, *35*(23), L23102. https://doi.org/10.1029/2008gl035798

Kirkwood, S., Chilson, P., Belova, E., Dalin, P., Häggström, I., Rietveld, M., and Singer W. (2006). Infrasound—the cause of strong polar mesosphere winter echoes?. *Ann. Geophys.*, *24*(2), 475–491. https://doi.org/10.5194/angeo-24-475-2006

Kirkwood, S., Belova, E., Dalin, P., Mihalikova, M., Mikhaylova, D., Murtagh, D., Nilsson, H., Satheesan, K., Urban, J., and Wolf, I. (2013). Response of polar mesosphere summer echoes to geomagnetic disturbances in the southern and northern hemispheres: the importance of nitric oxide. *Ann. Geophys.*, *31*(2), 333–347. https://doi.org/10.5194/angeo-31-333-2013

Kirkwood, S., Osepian, A., Belova, E., and Lee, Y. S. (2015). High-speed solar wind streams and polar mesosphere winter echoes at Troll, Antarctica. *Ann. Geophys.*, *33*(6), 609–622. https://doi.org/10.5194/angeo-33-609-2015

La Hoz, C., and Havnes, O. (2008). Artificial modification of polar mesospheric winter echoes with an RF heater: do charged dust particles play an active role?. *J. Geophys. Res.*, *113*(D19), D19205. https://doi.org/10.1029/2008JD010460

Lehtinen, M. S., and Huuskonen, A. (1996). General incoherent scatter analysis and GUISDAP. *J. Atmos. Terr. Phys.*, *58*(1–4), 435–452. https://doi.org/

10.1016/0021-9169 (95)00047-X https://doi.org/10.1016/0021-9169(95)00047-X

Li, H. L., Ge, S. C., Meng, L., Wang, M. Y., Rauf, A., and Ullah, S. (2021). Exploring the occurrence rate of PMSE-Es by Digisonde at Tromsø. *Earth Planet. Phys.*, *5*(2), 1–9. https://doi.org/10.26464/epp2021017

Liu, Y., Zhou, C., Xu, T., Tang, Q., Deng, Z. X., Chen, G. Y., and Wang, Z. K. (2021). Review of ionospheric irregularities and ionospheric electrodynamic coupling in the middle latitude region. *Earth Planet. Phys.*, *5*(5), 462–482. https://doi.org/10.26464/epp2021025

Lübken, F. J., Strelnikov, B., Rapp, M., Singer, W., Latteck, R., Brattli, A., Hoppe, U. P., and Friedrich, M. (2006). The thermal and dynamical state of the atmosphere during polar mesosphere winter echoes. *Atmos. Chem. Phys.*, *6*(1), 13–24. https://doi.org/10.5194/acp-6-13-2006

Mahmoudian, A., Mohebalhojeh, A. R., Farahani, M. M., Scales, W. A., and Kosch, M. (2017). Remote sensing of mesospheric dust layers using active modulation of PMWE by high-power radio waves. *J. Geophys. Res.*: *Space Phys.*, *122*(1), 843–856. https://doi.org/10.1002/2016JA023388

Næsheim, L. I., Havnes, O., and La Hoz, C. (2008). A comparison of polar mesosphere summer echo at VHF (224 MHz) and UHF (930 MHz) and the effects of artificial electron heating. *J. Geophys. Res.*: *Atmos.*, *113*(D8), D08205. https://doi.org/10.1029/2007JD009245

Nishiyama, T., Sato, K., Nakamura, T., Tsutsumi, M., Sato, T., Tanaka, Y. M., Nishimura, K., Tomikawa, Y., and Kohma, M. (2018). Simultaneous observations of polar mesosphere winter echoes and cosmic noise absorptions in a common volume by the PANSY radar (69.0°S, 39.6°E). *J. Geophys. Res.*: *Space Phys.*, *123*(6), 5019–5032. https://doi.org/10.1029/2017JA024717

Pinedo, H., La Hoz, C., Havnes, O., and Rietveld, M. (2014). Electron-ion temperature ratio estimations in the summer polar mesosphere when subject to HF radio wave heating. *J. Atmos. Sol.-Terr. Phys.*, *118*, 106–112. https://doi.org/10.1016/j.jastp.2013.12.016

Rapp, M., and Lübken, F. J. (2004). Polar mesosphere summer echoes (PMSE): review of observations and current understanding. *Atmos. Chem. Phys.*, *4*(11–12), 2601–2633. https://doi.org/10.5194/acp-4-2601-2004

Rapp, M., Latteck, R., Stober, G., Hofmann, P., Singer, W., and Zecha, M. (2011). First three-dimensional observations of polar mesosphere winter echoes: resolving space–time ambiguity. *J. Geophys. Res.*: *Space Phys.*, *116*(A11), A11307. https://doi.org/10.1029/2011JA016858

Rauf, A., Li, H. L., Ullah, S., Meng, L., Wang, B., and Wang, M. Y. (2018). Statistical study about the influence of particle precipitation on mesosphere summer echoes in polar latitudes during July 2013. *Earth Planets Space*, *70*(1), 108. https://doi.org/10.1186/s40623-018-0885-6

Rauf, A., Li, H. L., Ullah, S., Meng, L., Wang, B., and Wang, M. (2019). Investigation of PMSE dependence on high energy particle precipitation during their simultaneous occurrence. *Adv. Space Res.*, *63*(1), 309–316. https://doi.org/10.1016/j.asr.2018.09.007

Rietveld, M. T., Kohl, H., Kopka, H., and Stubbe, P. (1993). Introduction to ionospheric heating at Tromsø—I: experimental overview. *J. Atmos. Terr. Phys.*, *55*(4–5), 577–599. https://doi.org/10.1016/0021-9169(93)90007-L

Rietveld, M. T., Senior, A., Markkanen, J., and Westman, A. (2016). New capabilities of the upgraded EISCAT high-power HF facility. *Radio Sci.*, *51*(9), 1533–1546. https://doi.org/10.1002/2016RS006093

Rietveld, M. T., and Stubbe, P. (2022). History of the Tromsø ionosphere heating facility. *Hist. Geo Space Sci.*, *13*(1), 71–82. https://doi.org/10.5194/hgss-13-71-2022

Röttger, J., and La Hoz, C. (1990). Characteristics of polar mesosphere summer echoes (PMSE) observed with the EISCAT 224 MHz radar and possible explanations of their origin. *J. Atmos. Terr. Phys.*, *52*(10–11), 893–906. https://doi.org/10.1016/0021-9169(90)90023-G

Routledge, G., Kosch, M. J., Senior, A., Kavanagh, A. J., McCrea, I. W., and Rietveld, M. T. (2011). A statistical survey of electron temperature enhancements in heater modulated polar mesospheric summer echoes at EISCAT. *J. Atmos. Sol.-Terr. Phys.*, *73*(4), 472–482. https://doi.org/10.1016/j.jastp.2010.11.004

Scales, W. (2004). Electron temperature effects on small-scale plasma irregularities associated with charged dust in the Earth's mesosphere. *IEEE Trans. Plasma Sci.*, *32*(2), 724–730. https://doi.org/10.1109/tps.2004.826082

Scales, W. A., and Chen, C. (2008). On initial enhancement of mesospheric dust associated plasma irregularities subsequent to radiowave heating. *Ann. Geophys.*, *26*(8), 2265–2271. https://doi.org/10.5194/angeo-26-2265-2008

Senior, A., Mahmoudian, A., Pinedo, H., La Hoz, C., Rietveld, M. T., Scales, W. A., and Kosch, M. J. (2014). First modulation of high-frequency polar mesospheric summer echoes by radio heating of the ionosphere. *Geophys. Res. Lett.*, *41*(15), 5347–5353. https://doi.org/10.1002/2014GL060703

Shi, G. C., Hu, X., Yao, Z. G., Guo, W. J., Sun, M. C., and Gong, X. Y. (2021). Case study on stratospheric and mesospheric concentric gravity waves generated by deep convection. *Earth Planet. Phys.*, *5*(1), 79–89. https://doi.org/10.26464/epp2021002

Ullah, S., Li, H. L., Rauf, A., Meng, L., Wang, B., and Wang, M. Y. (2019). Statistical study of PMSE response to HF heating in two altitude regions. *Earth Planets Space*, *71*(1), 22. https://doi.org/10.1186/s40623-019-1007-9

Von Cossart, G., Fiedler, J., and Von Zahn, U. (1999). Size distributions of NLC particles as determined from 3-color observations of NLC by ground-based lidar. *Geophys. Res. Lett.*, *26*(11), 1513–1516. https://doi.org/10.1029/1999GL900226

Von Zahn, U., and Meyer, W. (1989). Mesopause temperatures in polar summer. *J. Geophys. Res.*, *94*(D12), 14647–14651. https://doi.org/10.1029/jd094id12p14647

Zeller, O., Zecha, M. Bremer, J. Latteck, R., and Singer, W. (2006). Mean characteristics of mesosphere winter echoes at mid- and high-latitudes. *J. Atmos. Sol.-Terr. Phys.*, *68*(10), 1087–1104. https://doi.org/10.1016/j.jastp.2006.02.015